Non-contact method to reduce contact problems between sample and electrode in dielectric measurements

High Voltage

Research Article

IET Journals
The Institution of Engineering and Technology

Non-contact method to reduce contact problems between sample and electrode in dielectric measurements

eISSN 2397-7264
Received on 15th November 2019
Revised 12th May 2020
Accepted on 28th May 2020
E-First on 15th July 2020
doi: 10.1049/hve.2019.0334
www.ietdl.org

Jing Hao[1] ✉, *Xiangdong Xu*[2], *Nathaniel Taylor*[1]

[1]*Electromagnetic Engineering, KTH Royal Institute of Technology, 100 44 Stockholm, Sweden*
[2]*Electric Power Engineering, Chalmers University of Technology, 412 96 Gothenburg, Sweden*
✉ *E-mail: jhao@kth.se*

Abstract: Dielectric response measurement is a widely used technique for characterising dielectric materials in terms of their capacitance and dielectric loss. However, the widely used approach with contact between samples and electrodes can in some cases limit the accuracy of the measurement. The authors introduce an easily realised electrode arrangement for non-contact measurements, which avoids these contact problems. The performance of the electrode arrangement in terms of the edge effect is assessed. The non-contact and contact methods are compared based on error-sensitivity analysis and experimental results. Differences are studied further, with attention to contact pressure. The non-contact method is also compared experimentally with the one-sided non-contact method. Air-reference measurements, comparing the sample to an air-gap for improved calibration, are used for all measurements. The results show that the non-contact method can be an alternative to reduce contact problems between the sample and electrodes, although error sensitivity can be higher when the non-contact method is used. The non-contact method can decrease the influence of the pressure applied to the sample compared to the contact method, and can also reduce the problem of poor contact that can arise from the absence of pressure in the one-sided non-contact method.

1 Introduction

Dielectric response measurement is a widely used method to assess the condition of high voltage equipment [1, 2]. It can be divided into time domain and frequency domain measurements. By performing frequency domain spectroscopy (FDS) measurements, the complex capacitance or complex permittivity can be determined [3].

A common way to perform FDS measurement on a material sample is to place the sample between two parallel electrodes, and then apply a sinusoidal voltage between the electrodes while measuring the current that flows between them. Some pressure is usually applied by gravity, a spring or other clamping, to ensure sufficient contact between the sample and electrode surfaces. This method is convenient and well established. However, there are several inherent deficiencies that may affect the reproducibility and the accuracy of results. One potential problem is related to the pressure applied by the electrodes on the sample. Either an excessive or an insufficient pressure will lead to contact problems, affecting the accuracy of the results [4]. An excessive pressure can change the sample's behaviour, particularly for samples with some kind of filler. An insufficient pressure will lead to small macro air gaps between the sample and electrode surfaces, forming current paths along the sample surface, which will yield a higher measured loss factor. The existence of the unwanted air gaps will also change results due to the additional air gaps connected in series with the sample. Another potential drawback of contact-based measurements is reactions at the sample/electrode interfaces. These reactions can increase the number of mobile charge carriers, leading to a conductivity that is beyond the level of the sample's intrinsic behaviour [5]. For example, in the ferric-ferrous redox reaction, an electron transfer takes place across the electrode interface, forming ferrous ions though the combination of ferric ions and electrons [6]. Experimental results in [7, 8] show that the materials of the electrode have an influence on the results of dielectric response measurements.

Several types of electrode arrangements have been introduced to improve measurements. To obtain good contact between the electrodes and sample, avoiding unintended air-gaps, a wide variety of electrode types has been used. Mercury, as a liquid metal, has been used in the past [9], but its toxicity limits its use now. Another alternative is the foil electrode which consists of a sheet of metal foil, for example tin, applied to either side of the sample usually with a thin film of wax or petrolatum to serve as an adhesive [10]. This has the advantages that it establishes good contact between the irregular sample and electrodes, and the very small thickness of the electrode reduces the error due to the field from the side of the electrode passing partially through the air and partially through the sample. However, some errors may result due to the wax or petrolatum in series with the sample and used to provide good adhesion contact with the sample [8]. A conducting substance can be directly applied to the sample surfaces by conductive paint or deposited metal (sputtered, vapour-deposited or spray-deposited electrodes), establishing intimate contacts between the sample and the coating [11, 12]. However, such electrodes are also not easily removed, which can prevent the use of the sample in further types of testing [13]. Besides this, diffusion can occur into the sample, and the surface resistance of the coating materials may affect results. Conductive rubber electrodes have been applied in many fields outside dielectric measurements because of the advantages of good elasticity and ageing resistance [14, 15]. Nevertheless, the high sensitivity of the conductive rubber to the pressure can be a problem in the FDS measurements, as the pressure can vary when using different electrode configurations or measuring different samples [16].

The electrodes discussed above can improve the contact area of electrodes on the sample to different extents, but they are not helpful for blocking reactions occurring at the interfaces. For avoiding reactions between the sample and electrodes, blocking electrodes that include an insulating layer on the surface of the electrode have been used. The insulating layers can effectively block the reactions between the sample and the electrode, but the insulating films will result in additional errors instead of improving signal analysis, unless the frequency-dependent dielectric properties of the thin films are accurately modelled [5].

In view of the problems associated with contacts between the sample and electrodes, it is tempting to eliminate the direct contacts. This is a long-established method in other disciplines that typically work with high frequency and low voltage [17]. A non-contact, or more strictly a one-sided non-contact, electrode

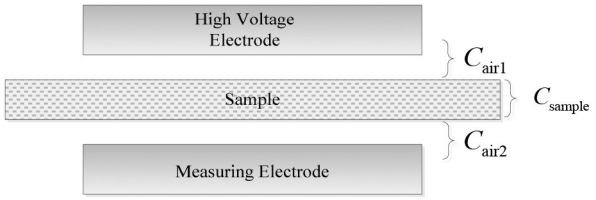

Fig. 1 *Sketch of the non-contact measurement*

arrangement for a high-voltage engineering application was introduced in [4]. In a measurement with this arrangement, the sample is placed on the lower electrode and separated from the upper electrode by an air gap. After the measurement, the measured capacitance will be compensated with the air gap capacitance in order to obtain the sample capacitance. A computer model of the field pattern around the electrodes and sample can be further used to improve the accuracy of the compensation by considering fringing fields [18]. Studies have analysed the sensitivity of the method to error sources [19], and the correction of the geometric influence [20, 21], and have used this method to measure the complex permittivity of silicone rubber [22]. However, the ideal contact-free situation has not been realised as the sample still needs to contact the lower electrode which will also probably lead to surface resistance and contact problems. The contact quality may indeed become worse at the lower electrode than in a contact-based arrangement, as there is no pressure applied from the upper electrode.

In this paper, an electrode arrangement is introduced to realise fully contact-free measurements within, intended primarily for the frequency range of 0.1 mHz–1 kHz. This electrode arrangement's fringing has been assessed by finite-element method (FEM). The error sensitivity of the non-contact method is compared by simulation with that of the conventional contact method. In addition, non-contact measurements are compared experimentally with contact and one-sided non-contact measurements.

2 Theory

2.1 Non-contact measurement

When a dielectric material is exposed to an electric field, a current is caused by two mechanisms in the material: polarisation and conduction. The polarisation includes several processes, such as electronic polarisation, ionic polarisation and so on. The conduction refers to the movement of charged particles that are not limited in the extent of their movement as are those in polarisation processes. The current through the dielectric material can be expressed by

$$i(t) = C_0\left[\frac{\sigma}{\varepsilon_0}v(t) + \varepsilon_\infty\frac{\mathrm{d}v(t)}{\mathrm{d}t} + \frac{\mathrm{d}}{\mathrm{d}t}\int_0^\infty f_{\mathrm{diel}}(\tau)v(t-\tau)\mathrm{d}\tau\right] \tag{1}$$

where C_0 is the geometrical capacitance of the sample, σ is the DC conductivity of the tested sample, ε_0 is the vacuum permittivity, ε_∞ is the relative permittivity at high frequency, $v(t)$ is the voltage applied on the sample and $f_{\mathrm{diel}}(t)$ is the dielectric response function.

Applying Fourier transformation to (1), the resultant current can be expressed in the frequency domain as a function of frequency

$$\begin{aligned} I(\omega) &= j\omega C_0\left[\varepsilon_\infty + \chi'(\omega) - j\left(\frac{\sigma}{\varepsilon_0\omega} + \chi''(\omega)\right)\right]V(\omega) \\ &= j\omega[C'(\omega) - jC''(\omega)]V(\omega) \end{aligned} \tag{2}$$

where the complex dielectric susceptibility $\chi^*(\omega) = \chi'(\omega) - j\chi''(\omega)$ is the Fourier transformation of the dielectric response function. If the dimensions of the sample are accurately known, the complex permittivity of the sample can be computed.

If the surfaces of the sample and electrodes are separated by air gaps as shown in Fig. 1, then the contact is avoided but additional capacitances of the air gaps are added in series with the sample.

The total measured capacitance $C^*_{\mathrm{total}}(\omega)$ between the electrodes, neglecting fringing, is then

$$\frac{1}{C^*_{\mathrm{total}}(\omega)} = \frac{1}{C^*_{\mathrm{air1}}(\omega)} + \frac{1}{C^*_{\mathrm{air2}}(\omega)} + \frac{1}{C^*_{\mathrm{sample}}(\omega)} = j\omega\frac{V(\omega)}{I(\omega)} \tag{3}$$

where $C^*_{\mathrm{air}i}$ is the complex capacitance of air gap i, with area $S_{\mathrm{air}i}$ and thickness $d_{\mathrm{air}i}$, leading to (4) if the air is assumed to have a relative permittivity of 1

$$C^*_{\mathrm{air}i}(\omega) = C^*_{\mathrm{air}i} = \varepsilon_0\frac{S_{\mathrm{air}i}}{d_{\mathrm{air}i}} \tag{4}$$

2.2 Air reference method

In this paper, the air reference method described in [4] is used to compensate instrument errors such as a poorly known value of the feedback admittance Y_{f}. The capacitance of the air C_{air} without sample inserted is measured and treated as a reference to eliminate the common instrument error factor between the capacitance of the sample C_{sample} and air C_{air} by dividing C_{sample} by C_{air}.

For deriving the permittivity of the sample, dimensions of the sample and the air gaps need to be accurately measured, including the thickness of the sample d_{sample} and the thickness of the two air gaps d_1 and d_2. With the use of the air reference method, the thickness of the reference air gap also should be known, which is the total of d_1, d_2 and d_{sample}. The total capacitance C_{tot} is the capacitance of two air gaps (C_1, C_2) and the sample C_{sample} connected in series, as shown in (5). Therefore, the capacitance of the sample can be derived by (6). By using the air reference method, the complex permittivity of the sample can be calculated by (7)

$$\begin{aligned} C_{\mathrm{tot}} &= \frac{1}{1/C_{\mathrm{sample}} + 1/C_1 + 1/C_2} \\ &= \frac{C_{\mathrm{sample}}C_1C_2}{C_1C_2 + C_{\mathrm{sample}}C_2 + C_{\mathrm{sample}}C_1} \end{aligned} \tag{5}$$

$$C_{\mathrm{sample}} = \frac{1}{1/C_{\mathrm{tot}} - 1/C_1 - 1/C_2} \tag{6}$$

$$\varepsilon^*_{\mathrm{r}} = \varepsilon'_{\mathrm{r}} - j\varepsilon''_{\mathrm{r}} = \frac{C_{\mathrm{sample}}}{C_{\mathrm{airref}}}\frac{d_{\mathrm{sample}}}{d_1 + d_2 + d_{\mathrm{sample}}} \tag{7}$$

3 Measurement design

3.1 Electrode arrangement

We designed an electrode arrangement for non-contact measurements with the performed range of 0.1 mHz–1 kHz [23]. This arrangement consists of two similar electrode assemblies (see Fig. 2*a*), each similar to the conventional measurement electrode with a guard ring, which means that this non-contact arrangement can be realised by adjusting the current electrode arrangement used in most labs without complex manufacture.

Those two electrode assemblies together form a four-electrode arrangement, of a measuring and guard electrode and a high-voltage and support electrode. The internal structure is shown in Fig. 2*b* which shows the cross-section along the surface 'A' marked in Fig. 2*a*, omitting the bolts through the ring electrodes and frames. The measuring and the high-voltage electrodes have 27 mm radius, the guard and the support electrode have internal and external radii of 30 and 40 mm, and all four electrodes are 5 mm in the axial direction. For a non-contact measurement, thin insulating films are inserted to hold the guard and support electrodes further from their baseplates, causing these ring electrodes to extend beyond the measuring and high-voltage electrodes that they surround. The sample is clamped between the guard electrode and

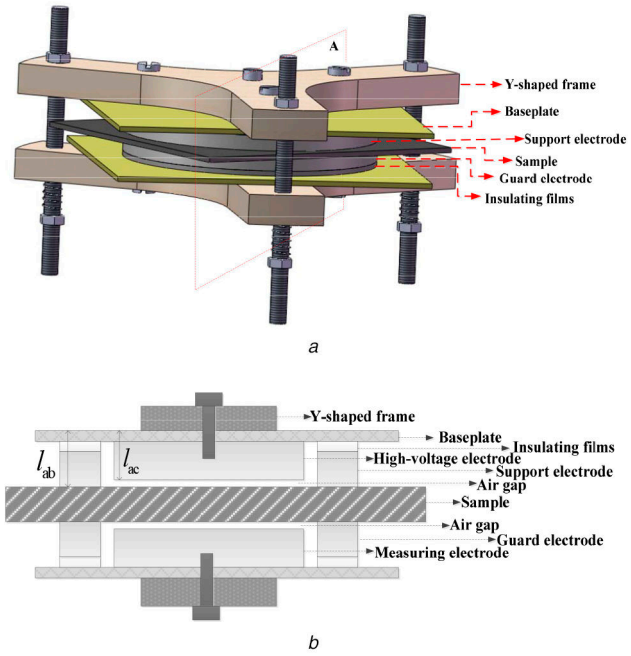

Fig. 2 *Sketch of the non-contact electrode arrangement*
(a) 3D structure of the electrode arrangement, ***(b)*** Cross-section through the surface A

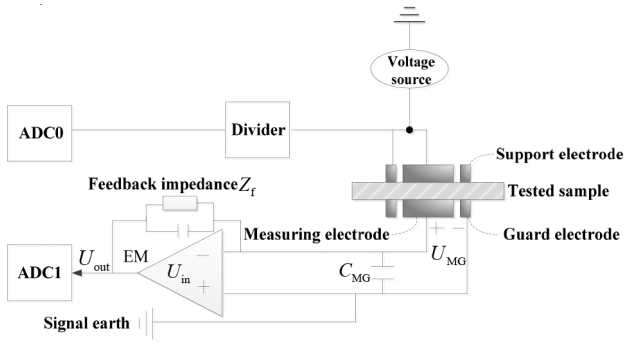

Fig. 3 *Diagram of the main parts in the system of electrodes and FDS instrument*

the support electrode, leaving an air gap between the sample and the inner electrode surfaces in the direction of the electric field.

The four electrodes are fixed by conductive bolts to their own baseplates that have a thickness of 1.5 mm and Y-shaped frames with a thickness of 10 mm. The two parts of the electrode are fixed together by long bolts through the Y-shaped frames, and then screwed by nuts. In the measurement, the support electrode is connected with the high-voltage electrode by connecting two bolts. There is a spring setting in each long bolt, which can be used to change the pressure applied to the sample. This electrode arrangement can be placed vertically to avoid the case where a soft sample droops under gravity and thereby forms unwanted contacts with an electrode.

3.2 Measurement systems

Besides an electrode arrangement, a measurement of dielectric response requires an instrument to measure the voltage and current. The commercial FDS instrument IDAX300 was used in this work to apply and measure a voltage and to measure the resulting current through the sample. The current into the 'measure' terminal is converted to a voltage signal through the electrometer EM and then measured in the analogue–digital converter ADC1. The main parts in this setup are shown in Fig. 3.

The electrometer's feedback is through a parallel capacitor and resistor. The values of these components are chosen for each measured voltage amplitude and frequency, in order to keep the output voltage as high as possible within the limits of the analogue–digital conversion. The instrument used in this work has nine available resistances, at all decades from 100 Ω to 10 GΩ, and six capacitances from 100 pF to 10 μF.

3.3 Experimental procedure

The experimental procedures mainly include processing samples, adjusting the electrodes, measuring dimensions, and performing the capacitance measurements. Before the measurements, each sample was cleaned by rinsing it with isopropanol, and dried in a drying oven for 24 h. Then, the sample's thickness d_{sample} was measured, which was an average value of ten different locations. In order to avoid deformation of the sample by the micrometer, the sample was clamped between two polycarbonate plates each of thickness 1.00 mm, and the total thickness was measured with a screw micrometer, then the measured thickness of the polycarbonate was subtracted from the total thickness measured by the micrometer.

In cases where the conventional contact measurement was carried out for comparison, this measurement was the first to be performed after measuring the sample thickness. In this measurement, the electrodes were applied to the sample with moderate pressure from the three bolts holding the electrodes together. In order to have an air-reference measurement for the contact-based material measurement, the sample was then removed, and small pieces of sample or rings from the same batch were placed between the guard and support electrodes in order to make the separation similar to how it was in the material measurement conditions, then the capacitance of this arrangement was measured.

For the non-contact measurement, thin insulating films were inserted between the annular outer electrodes (guard and support) and their baseplates (Fig. 2), moving these electrodes' surfaces further from the baseplate than the surfaces of the inner electrodes (measuring and high voltage). For calculating the permittivity of the sample from the measured capacitance, the thickness of the air gaps that in series with the sample is needed. This was determined as the difference between l_{ab} and l_{ac}, shown in Fig. 2*b*, by measuring the mean values over ten positions using a screw micrometer. The thickness of each air gap was taken as the difference between those two distances for the electrodes at that side of the sample. The sample was then inserted between the electrodes, and the springs were adjusted to the length to apply the planned pressure to the sample. After the non-contact measurement, the sample was replaced by sample pieces between just the guard and support electrodes, in order to measure the air-reference capacitance for the non-contact measurements.

Measurements were repeated according to the previous order of contact measurement followed by non-contact measurement, to evaluate the reproducibility of measurements. The flowchart of the experimental procedure is shown in Fig. 4.

4 Evaluations of the non-contact method

Reliability, precision and error sensitivity are important aspects of the measurement, and should be assessed. This section evaluates the non-contact electrode arrangement and the non-contact method by simulation.

4.1 Edge effect

Edge effect or 'fringing' refers to the electrostatic flux spreading out at the edges of the electrodes and air, including a different area of the sample compared to that of the electrode. Although the guard ring effectively increases the homogeneity of the electric field at the edge of the electrode, the fringing problem is not totally solved. At the boundary of the electrode, the electrostatic flux that is partly through the sample and partly through the air will still have an effect both on the amplitude and the phase of the complex capacitance. It is shown in [24] that for the measurement cell design, involved materials, potential distribution and the test specimen height are factors that influence the fringing. For the four-electrode arrangement illustrated above, the fringing should be assessed considering those aspects.

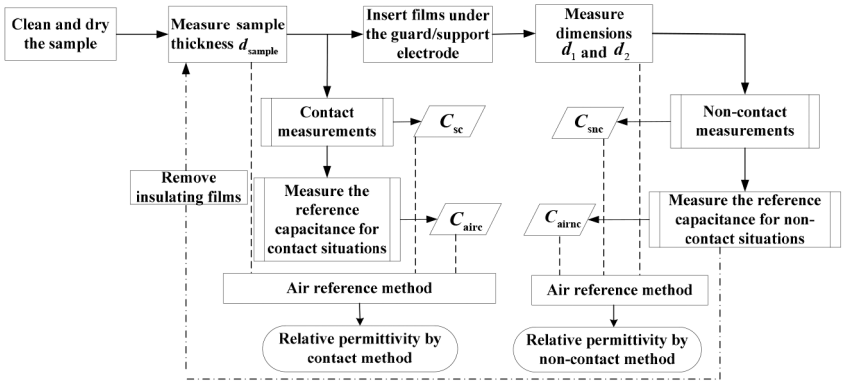

Fig. 4 *Flowchart of the experimental procedure*

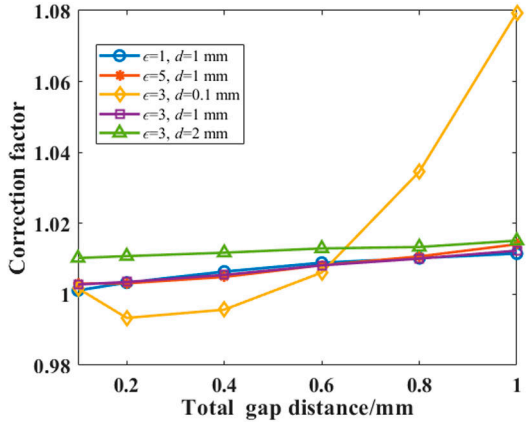

Fig. 5 *Correction factors of the permittivity with different total air gap distance, relative permittivity values and sample thickness (the potential of the support electrode is set to be the same as for the high-voltage electrode. ε: the set permittivity; d: the sample thickness)*

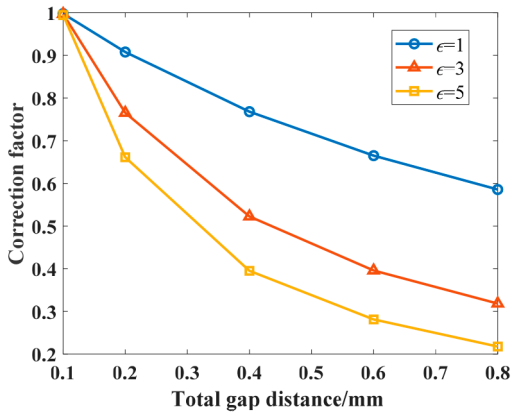

Fig. 6 *Correction factors of the permittivity with different total air gap distance and relative permittivity values (the potential of the support electrode is connected to ground. ε: the set permittivity)*

FEM calculations were used to study the edge effect in the electrode arrangement introduced in Section 3.1. This was done by three-dimensional electrostatic simulation in Comsol Multiphysics. In the simulation, the potential of the high-voltage electrode and the support electrode is set to be 140 V (voltage source), and the measuring electrode and the guard electrode is set to be 0 V. The homogeneity of the electric field and the edge effect is assessed by the correction factors of the permittivity, which is the ratio $\varepsilon_{sim}/\varepsilon$. Here, ε is the permittivity set for the sample material in the simulation, and ε_{sim} is the permittivity calculated from the simulated current at the measuring electrode by the method described in Section 2.1 for processing measurement results. The correction factors as a function of the total air gap distance with consideration of the relative sample permittivity and sample thickness are shown in Fig. 5. Except for the case when the sample thickness is 0.1 mm, the simulated permittivity deviates more from the set values with increased air gap distance. The sample permittivity makes a negligible difference to the results, while the sample thickness (which affects the air-gap as the total electrode spacing is kept constant) has a significant effect on the results. Especially, the correction factors show that the deviation of the permittivity goes through a maximum value and a minimum value when the total thickness increases from 0.1 to 1 mm with a sample thickness of 0.1 mm. If the sample thickness is bigger than the total gap distance and the support electrode is connected to the voltage source, the error caused by the edge effect does not exceed 1.5% relative error even if the total air gap distance goes up to 1 mm. Therefore, the results can be free from correcting in this case. The influence of the sample radius has also been estimated and the results show that the influence of the sample radius can be ignored if the radius of the sample is bigger than that of the measuring electrode.

Another alternative is to connect the support electrode with the ground. The corresponding correction factors with different air gap distance and sample permittivity values for this case are shown in Fig. 6.

The results show that the simulated permittivities in this situation are significantly smaller than the set permittivities, and the correction factors are more sensitive to the air gap distances and sample permittivity compared to the case when the support electrode is connected to the voltage source. Therefore, this alternative is not used in this work.

4.2 Error sensitivity analysis and simulation

The error sensitivity is the extent to which the result of the measurement is affected by the variation of an input or system parameter from its believed value. When measuring a material permittivity, the sample thickness and area, the capacitance (impedance) measurement, and further details of the test cell, e.g. fringing, are all relevant, and all introduce uncertainty in the result. It is of interest to study how the non-contact type of measurement affects this sensitivity. The measurement errors can be classified by either systematic error or random error. Most systematic errors, such as the calibration error with constant error factor, can be eliminated by using the air reference method. Therefore, the random errors are mainly discussed in this section.

4.2.1 Error sensitivity analysis: The error sensitivity with the consideration of errors in the thickness of air gaps and sample has been discussed in detail in [4]. In this paper, the errors appearing in capacitance measurements are considered. Since the capacitance calculation involves the ratio of complex current and voltage, errors of scaling or phase shift of either of these quantities can be represented as errors of just one of these quantities. Based on this, this sensitivity analysis can be simplified by assessing sensitivity under the effect of amplitude and phase shift errors of the resultant current, as well as the added noise in the measured current.

The capacitance of the tested sample with the area S, relative permittivity ε_r and thickness d_{sample} can be expressed as

$$C_{\text{sample}} = \varepsilon_r \varepsilon_0 \frac{S}{d_{\text{sample}}} \tag{8}$$

where ε_0 is the vacuum permittivity. In the contact measurement, the capacitance between the measuring electrode and the high-voltage electrode C_c is exactly the capacitance of the sample. In the non-contact measurements, the capacitance, consisting of the sample and air gaps with a total thickness of d_{air} connected in series, is shown as

$$C_{\text{nc}} = \frac{\varepsilon_r \varepsilon_0 S}{d_{\text{sample}} + \varepsilon_r r d_{\text{sample}}} \tag{9}$$

where

$$r = \frac{d_{\text{air}}}{d_{\text{sample}}} \tag{10}$$

Here, it is assumed that the amplitude error factor is k_1 and the phase shift factor is k_2, then the error factor can be expressed as

$$K = (1 + k_1) \cdot e^{jk_2} \tag{11}$$

The measured currents through the sample using the contact and the non-contact measurements can be calculated by (12) and (13), respectively

$$I_{\text{c\_error}} = j\omega C_c V K \tag{12}$$

$$I_{\text{nc\_error}} = j\omega C_{\text{nc}} V K \tag{13}$$

In the contact measurement, the measured capacitance $C_{\text{c\_error}}$ considering the error factor can be calculated by (14), which is equal to the measured sample capacitance considering errors $C_{\text{sc\_error}}$. It can be found that the error sensitivity of contact measurements is equal to the error coefficient K

$$C_{\text{sc\_error}} = C_{\text{c\_error}} = \frac{I_{\text{c\_error}}}{j\omega V} = C_c K = C_{\text{sample}} K \tag{14}$$

On the other hand, the tested capacitance under the effect of errors in the non-contact measurement is

$$C_{\text{nc\_error}} = \frac{I_{\text{nc\_error}}}{j\omega V} = C_{\text{nc}} K = \frac{\varepsilon_r \varepsilon_0 S}{d_{\text{sample}} + \varepsilon_r r d_{\text{sample}}} \cdot K \tag{15}$$

The tested capacitance of the sample after compensating the air gaps can be expressed as (16), showing the deviation coefficient of non-contact measurement is $\frac{K}{r\varepsilon_r - Kr\varepsilon_r + 1}$ when the error factor is K

$$C_{\text{snc\_error}} = C_{\text{sample}} \frac{K}{r\varepsilon_r - Kr\varepsilon_r + 1} \tag{16}$$

The relative error sensitivity of the contact and non-contact measurements is the ratio of two deviation factors, shown as

$$K_{\text{relative}} = 1 + r\varepsilon_r(1 - K) \tag{17}$$

It can be deduced that an amplitude measurement error with the coefficient k_1 can lead to an amplitude error in the final capacitance with the coefficient that is bigger than k_1 by using the non-contact method, and the situation is the same with regard to the phase error. In contrast, the contact method transfers amplitude and phase errors in the impedance measurement directly into corresponding errors in the calculated sample capacitance.

For comparing error sensitivity of the two methods reacting to the noise, the current through the sample can be expressed by (18) and (19) for the contact and the non-contact methods, respectively

$$I_{\text{c\_noise}} = j\omega C_c V + k_{\text{random}} \tag{18}$$

$$I_{\text{nc\_noise}} = j\omega C_{\text{nc}} V + k_{\text{random}} \tag{19}$$

Similarly, the measured capacitance in the contact measurements and the non-contact measurements considering the influence of noise can be expressed by (20) and (21), respectively. The measured capacitance in the contact measurements is the measured sample capacitance. In contrast to the scaling errors, the effect of additive noise on the measured capacitance in the contact measurements depends on the voltage source and the measurement frequency, besides the properties of the noise itself. The error caused by the noise increases with the decrease of the frequency and the amplitude of the voltage source

$$C_{\text{sc\_noise}} = C_{\text{c\_noise}} = C_{\text{sample}} + \frac{k_{\text{random}}}{j\omega V} \tag{20}$$

$$C_{\text{nc\_noise}} = C_{\text{nc}} + \frac{k_{\text{random}}}{j\omega V} \tag{21}$$

Further, the measured capacitance of the sample in the non-contact measurements with the influence of noise can be obtained by compensating the air gaps, as shown in (22). It is worth noting that the sample capacitance measured by non-contact measurements without the influence of the noise is $\frac{C_{\text{air}} \cdot C_{\text{nc}}}{C_{\text{air}} - C_{\text{nc}}}$, which is a component of the first term on the right side of (22). Comparing (22) with (20) further, it is deduced that the noise only influences the amplitude of the imaginary part of the capacitance with the use of the contact measurements, while influences both the phase and amplitude of the measured capacitance by using non-contact measurements

$$C_{\text{snc\_noise}} = \frac{C_{\text{air}} \cdot C_{\text{nc}}}{C_{\text{air}} - C_{\text{nc}} - \frac{k_{\text{random}}}{j\omega V}} + \frac{k_{\text{random}}}{j\omega V\left(1 - \frac{C_{\text{nc}}}{C_{\text{air}}}\right) - \frac{k_{\text{random}}}{C_{\text{air}}}} \tag{22}$$

4.2.2 Simulation: Based on the analysis above, the following simple numerical simulation compares the influence of errors on the results obtained by contact measurements and non-contact measurements. It is assumed, purely as an example, that the polarisation of the sample has a Debye response. The complex permittivity with the consideration of the prompt capacitance ε_∞ and DC conductivity σ can be expressed as

$$\varepsilon^*_{\text{sample}} = \varepsilon_\infty + \frac{\varepsilon_s - \varepsilon_\infty}{1 + j\omega\tau} + \frac{\sigma_{\text{dc}}}{j\omega\varepsilon_0} \tag{23}$$

In the simulation, the dielectric properties of the sample material are $\varepsilon_\infty = 2$, $\varepsilon_s = 6$, $\tau = 2$ s, $\sigma_{\text{dc}} = 1 \times 10^{-11}$S/m and its thickness is 2 mm. The radius of the sample is 30 mm, and the field is assumed to have no fringing, so that a circuit model can be used. The two air gaps in the non-contact measurements are each 0.2 mm. For the errors, we assume $k_1 = 1 \times 10^{-2}$, $k_2 = 4 \times 10^{-3}$ and k_{random} is a series of random values from -1.5×10^{12} to 1.5×10^{12}. The simulation results obtained by the contact method and the non-contact method considering different error types are compared with the true results, as shown in Figs. 7–9.

The noise and the slight error in measuring the amplitude have a slight effect on the relative permittivities obtained by contact measurements, but they clearly influence the results of non-contact measurements, mainly at low frequencies. This is because of the bigger loss angle in low frequencies, which can lead to a bigger error under the same amplitude error or the same extent of random errors in measured results compared to a smaller angle in high frequencies. For the influence of the phase shift error, both the results obtained by the contact method and the non-contact method are affected, with deviation mainly exists in the lowest and highest frequency range, as shown in Fig. 8. The non-contact method gives a higher deviation than the contact method. The results have been

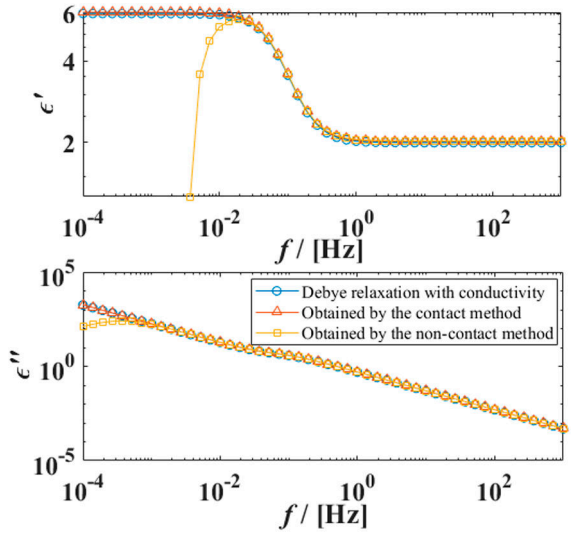

Fig. 7 *Complex permittivities of the sample with the effect of the amplitude error*

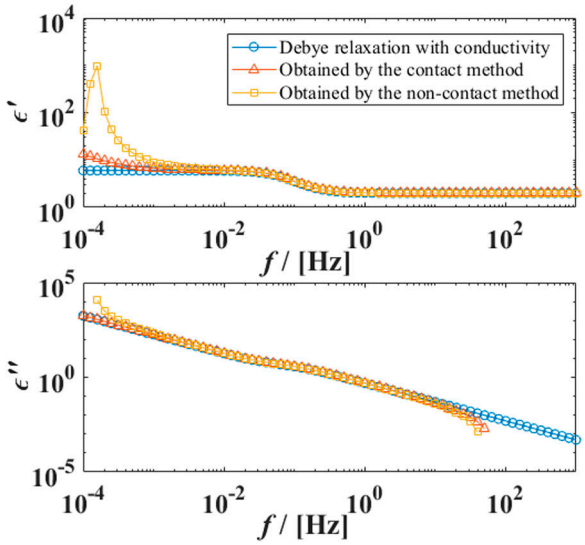

Fig. 8 *Complex permittivities of the sample with the effect of the phase shift error*

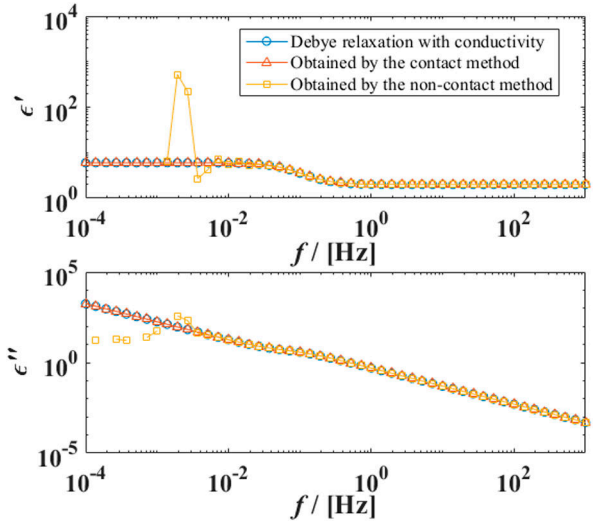

Fig. 9 *Complex permittivities of the sample with the effect of the noise*

used to estimate the lowest frequency limit for both real and imaginary permittivities with the threshold relative error of 5%. The approximate frequency limits for different types of errors with different values are shown in Table 1. The highest frequency limit in the imaginary part of permittivity caused by phase shift is not considered here.

For decreasing the deviation, well-calibrated measurement instruments are important. Good shielding and guarding are necessary. In addition, using the air reference method can effectively eliminate the deviation caused by systematic errors.

5 Results and discussions

The non-contact method was compared to both contact and one-sided non-contact method, using air-reference in both cases. Four types of the sample were used in the tests: polycarbonate, PVC (polyvinyl chloride), epoxy with 60% quartz powder and high temperature vulcanised (HTV) silicone rubber. They are examples of polymers with, respectively, low loss, significant loss, rough surfaces and soft surfaces.

5.1 Comparisons with contact method

The tested samples were both measured by using contact and non-contact measurements. Two influences were considered: the pressure applied to the sample, and control of the FDS instrument to lock the feedback selection to be the same for each sample and reference pair. The electrode configuration in Fig. 2 and the measurement system in Fig. 3 were used, following the procedures presented in Fig. 4. In order to eliminate the systematic errors by using the air reference method, the instrument's settings at each frequency, including its choice of feedback components, should be the same between the measurements on the sample and on the air-reference. Here, the relative permittivity of the PVC and the polycarbonate obtained with the feedback sequence locked between each sample/air-reference pair of measurements is compared with that obtained in auto mode where the feedback components are selected independently between different measurements.

5.1.1 Polyvinyl chloride: The thickness of the PVC is 1.00 mm, and the thicknesses of the two air gaps in the non-contact measurement are 0.115 and 0.11 mm. The complex permittivity of the PVC measured using the contact method and the non-contact method are compared in Fig. 10. Comparing the results obtained by the contact method and the non-contact method, it shows that the real part of the permittivity obtained by the non-contact method is bigger than that obtained by the contact method. For the imaginary permittivity, the values in the low frequencies for non-contact measurements are smaller than values for contact measurements, possibly because the loss caused by the surface conductivity has been decreased in the non-contact measurements. By locking feedback, the air reference method can effectively eliminate jumps that otherwise happened at 0.46 and 0.046 Hz, and also smooth the curve.

5.1.2 Polycarbonate: The permittivity of the polycarbonate measured by the contact and the non-contact measurement with the feedback locked and unlocked is compared in Fig. 11. The thickness of the polycarbonate is 1 mm, and the thicknesses of the two air gaps are 0.16 and 0.19 mm. Comparing the results obtained by the contact and the non-contact methods, it is seen that the real part of the permittivity obtained by the non-contact measurement is smaller than that obtained by the contact measurement, while the imaginary permittivity of the non-contact measurement is bigger than that of the contact measurement. For the imaginary part of the permittivity, the data obtained by contact measurements are flat in the range from 1000 to 0.01 Hz, while the results obtained by the non-contact measurement have a relaxation peak in this range. From 0.01 to 0.001 Hz, the results obtained by the non-contact method have an obvious increase, while that measured by the contact method decreases sharply to the negative.

The results show again the importance of locked feedback. There are also several points go down to negative in the imaginary part of the permittivity. Using locked feedback eliminates the negative points and forms a relatively smooth curve in the frequencies of 220, 110, 22 and 0.001 Hz. The reason why jumps

Table 1 Estimation of the low frequency limit for 5% relative error

k_1	1.4×10^{-4}	5×10^{-3}	1.0×10^{-2}	2×10^{-2}	5.0×10^{-2}
$f_{\text{lim\_real}}$	4.0×10^{-3}	8.6×10^{-3}	1.2×10^{-2}	1.6×10^{-2}	—
$f_{\text{lim\_imag}}$	1.4×10^{-4}	6.3×10^{-4}	1.2×10^{-3}	8.6×10^{-2}	—
k_2	2.0×10^{-4}	5.0×10^{-4}	1.0×10^{-3}	4.0×10^{-3}	1×10^{-2}
$f_{\text{lim\_real}}$	4.0×10^{-4}	1.0×10^{-3}	1.8×10^{-3}	7.4×10^{-3}	2.2×10^{-2}
$f_{\text{lim\_imag}}$	1.4×10^{-4}	3.4×10^{-4}	7.4×10^{-4}	2.9×10^{-3}	6.3×10^{-3}
k_{random}	1×10^{-14}	1.0×10^{-13}	5.0×10^{-13}	1.0×10^{-12}	1×10^{-11}
$f_{\text{lim\_real}}$	4.7×10^{-4}	1.2×10^{-3}	2.2×10^{-3}	4.6×10^{-3}	1.4×10^{-2}
$f_{\text{lim\_imag}}$	2.2×10^{-4}	4.7×10^{-4}	1.4×10^{-3}	2.2×10^{-3}	4.6×10^{-3}

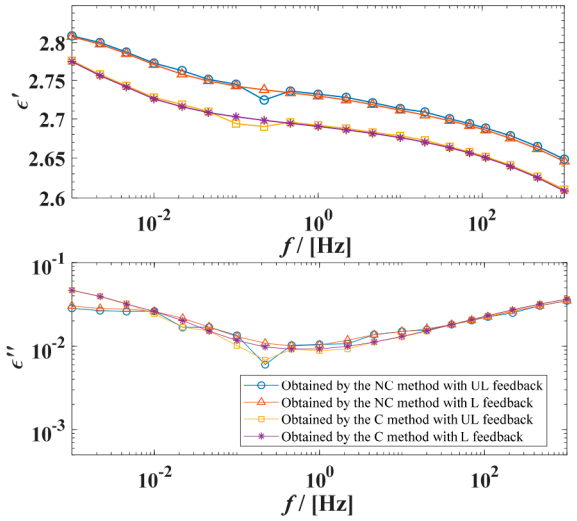

Fig. 10 *Complex permittivities of the PVC (NC: non-contact; C: contact; UL: unlocked feedback; L: locked feedback)*

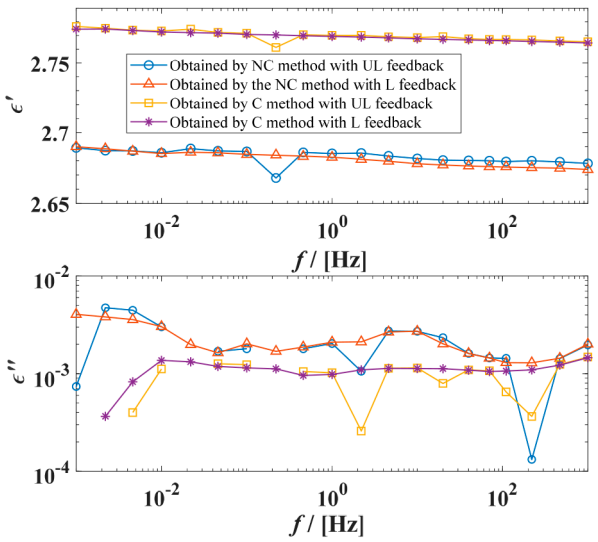

Fig. 11 *Complex permittivities of polycarbonate (NC: non-contact; C: contact; UL: unlocked feedback; L: locked feedback)*

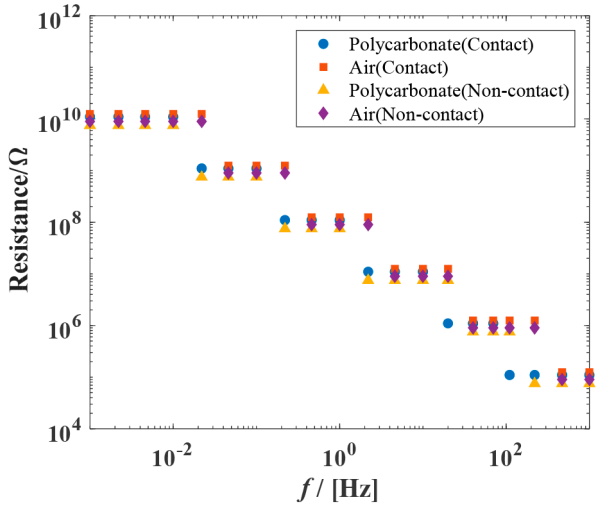

Fig. 12 *Resistance of the feedback used for measuring polycarbonate in auto mode*

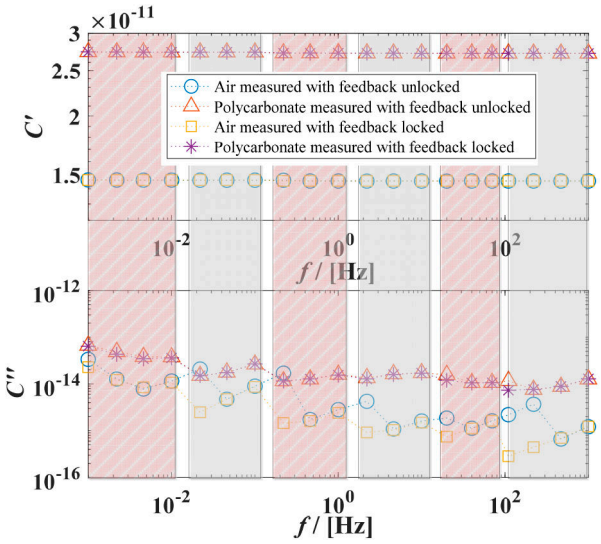

Fig. 13 *Capacitances of the reference air and the polycarbonate in the non-contact measurements with feedback locked and unlocked*

happen can be understood by comparing the resistance of the feedback (each resistance is an integer power of ten, but extra values were added for distinguishing) used for measuring the reference air and the sample in auto mode, as shown in Fig. 12. It can be seen the resistance sequence used for the sample is not the same as the sequence for the corresponding reference air in auto mode. In this case, the systematic errors of the feedback components cannot be eliminated, and the superposition of errors in two pairs of feedback components can even lead to a bigger error in the measured capacitance. The reason why locking feedback can eliminate the jumps can be further explained by comparing capacitances of the sample and the reference air measured in auto mode and feedback locked conditions. Fig. 13 shows capacitances measured by the non-contact measurements with the feedback locked and unlocked: the curves are divided into several parts using shading and the same resistance is used in each shaded area in feedback locked mode. It can be found that there are jumps in the measured capacitance every three or four frequency points, form a sawtooth curve. Comparing Figs. 12 and 13, it is seen that the jumps happen when the resistance of the feedback shifts from one value to another value, and the curve is relatively continuous when the capacitances are measured using the same feedback. If the feedback is not fixed in the measurements, the frequencies where jump points happen in the measurement of

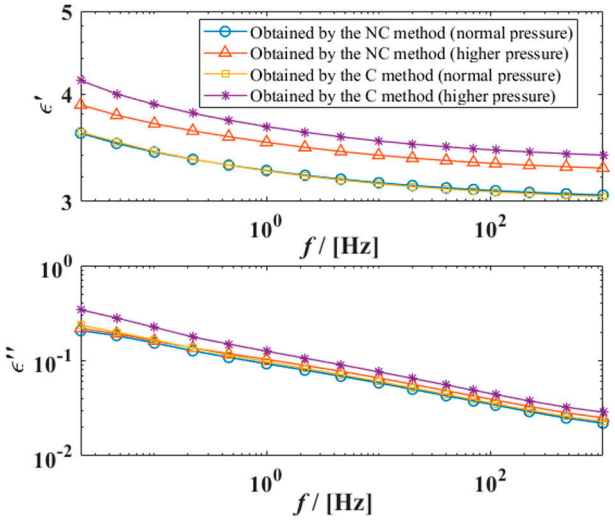

Fig. 14 *Complex permittivities of the epoxy with 60% quartz powder with different pressure (NC: non-contact; C: contact)*

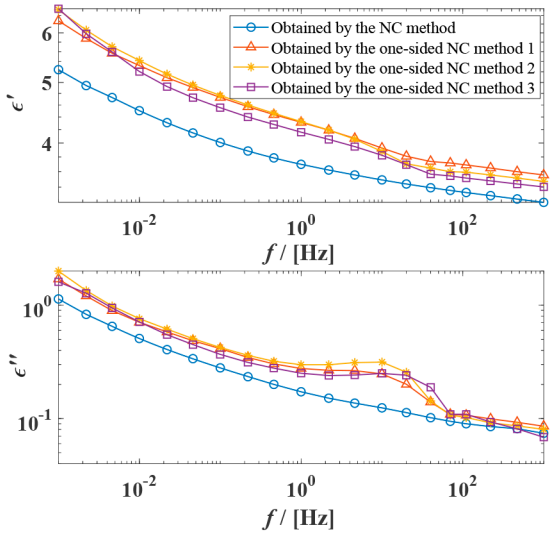

Fig. 15 *Complex permittivities of HTV silicone rubber*

polycarbonate cannot correspond to that in the measurement of the reference air. In this situation, the systematic errors are combined rather than equalised. If the feedback sequence is fixed to be the same between the measurement of the polycarbonate and the measurement of the reference air, the plot of the polycarbonate and the reference air coincide with each other. After locking the feedback, the variation trends of the sample and the reference air are controlled to be similar, so the air reference can effectively decrease the errors caused by systematic errors.

5.1.3 Influence of the pressure: The results of the FDS measurements are influenced by the contact situations between electrode surfaces and sample surfaces to some extent. The contact situation is partially determined by the pressure applied to the sample by the electrodes. A high pressure can reduce the small local gaps between the electrode and the sample, but it can deform the sample or change the thickness of the sample. A low pressure can avoid the deformation of the sample from the electrodes, but lacking sufficient pressure between the sample and the electrodes can be a problem with additional unintended gaps. The non-contact method has the advantage of avoiding contacts between the effective area of the sample and the electrodes, avoiding the contact problems occurring in the contact measurements.

Here, the influences of the pressure on the contact and the non-contact measurements are compared. The epoxy with 60% quartz powder is used as the tested sample, which has rough surfaces. The non-contact and the contact measurements are both performed

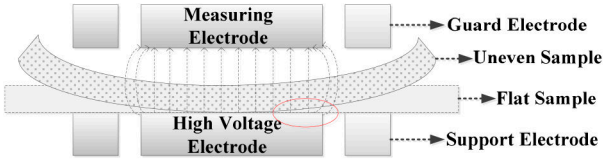

Fig. 16 *Sketch of the non-contact measurement when the sample is uneven*

under low pressure (around 20 N) and high pressure (around 120 N), respectively. The thickness of the sample is 2.15 mm, and the thickness of air gaps in non-contact measurement is 0.295 and 0.17 mm, respectively. The results are shown in Fig. 14. It is seen that the non-contact measurement is less influenced by the pressure applied to the sample compared with the contact measurement. The relative errors are within the range of 7–8% in the real part and 11–15% in the imaginary part by using the non-contact method. The errors are probably due to the spacing change caused by the high pressure between the guard electrode and the support electrode which is not fully taken into account when calculating permittivity. The relative errors with the use of the contact method are more significant, which are in the range of 4–14% in the real part, and 25–45% in the imaginary part.

5.2 Comparisons with one-sided non-contact method

Both the non-contact measurements and the one-sided non-contact measurements discussed in [4] were used for measurements on HTV silicone rubber. For the one-sided non-contact measurement, the electrode arrangement in Fig. 2 was used, with the upper electrode fixed by the nuts on the screws to give a chosen thickness of the air gap above the sample: refer to [4] for more detail about the procedure. The thickness of the silicone rubber is 2.00 mm. The thickness of the air gap is 0.45 mm in the one-sided non-contact measurements, and the thickness of the two air gaps in the non-contact measurements is 0.27 and 0.335 mm, respectively. The relative permittivities obtained by both methods are presented in Fig. 15. Both the real and imaginary parts of permittivity obtained by the one-sided non-contact method are bigger than the values from the non-contact method. This is probably caused by the rubber not lying so flat, due to the absence of pressure from the upper electrode, leading the electric lines to go through a bigger area of the sample, as shown in Fig. 16. In addition, there is an extra relaxation peak in high frequency by using the one-sided non-contact measurement, which may be caused by the bulk capacitance and surface resistance of the sample in regions with poor electrode contact as shown encircled in Fig. 16. The relaxation peak appearing in the one-sided non-contact measurement changes in amplitude and frequency when the sample is removed and placed again in the cell for repeated measurements, as shown in Fig. 15. Results from the non-contact method do not show this peak and are more consistent between repetitions. This observation supports the explanation of the extra relaxation peak as an artefact of the contact with the electrode.

6 Conclusion

In this paper, the non-contact method is introduced to perform FDS measurements using a new electrode arrangement that is simple to fabricate. The electrode arrangement was evaluated considering the edge effect. FDS measurements were carried out to study the influence of fixing the instrument's feedback and of the pressure applied to the sample by the electrodes. The evaluation and the analysis by simulations and experiments show that the non-contact method can be an alternative to reduce contact problems between the sample and electrodes, although error sensitivity can be higher when the non-contact method is used. Compared with the contact measurement, the non-contact measurement decreases the influence of the surface conductivity and the pressure applied to the sample. It can also decrease the problem in the one-sided non-contact measurements that can arise due to the absence of pressure from the upper electrode. The air reference method used with locked feedback components is effective in reducing systematic errors in the values of feedback components.

7 Acknowledgments

Jing Hao thank the China Scholarship Council (CSC File No. 201700260216) for its financial support of her studies in Sweden, and also thank Chalmers University of Technology for providing laboratory facilities and support during a research visit.

8 References

[1] Yang, L., Chen, J., Wang, S.*, et al.*: 'Dielectric response measurement of oil-paper insulation based on system identification and its time-frequency-domain conversion method', *IEEE Trans. Dielectr. Electr. Insul.*, 2018, **25**, (5), pp. 1688–1698

[2] Gao, J., Yang, L., Wang, Y.*, et al.*: 'Condition diagnosis of transformer oil-paper insulation using dielectric response fingerprint characteristics', *IEEE Trans. Dielectr. Electr. Insul.*, 2016, **23**, (2), pp. 1207–1218

[3] Setayeshmehr, A., Fofana, I., Eichler, C.*, et al.*: 'Dielectric spectroscopic measurements on transformer oil-paper insulation under controlled laboratory conditions', *IEEE Trans. Dielectr. Electr. Insul.*, 2008, **15**, (4), pp. 1100–1111

[4] Xu, X., Bengtsson, T., Blennow, J.*, et al.*: 'Enhanced accuracy in dielectric response material characterization by air reference method', *IEEE Trans. Dielectr. Electr. Insul.*, 2013, **20**, (3), pp. 913–921

[5] Richert, R.: 'Insulated electrodes for eliminating conductivity in dielectric relaxation experiments', *Eur. Phys. J. B*, 2009, **68**, (2), pp. 197–200

[6] Sato, N.: '*Electrochemistry at metal and semiconductor electrodes*' (Elsevier, Amsterdam, Netherlands, 1998)

[7] Rogti, F., Ferhat, M.: 'Maxwell–Wagner polarization and interfacial charge at the multi-layers of thermoplastic polymers', *J. Electrost.*, 2014, **72**, (1), pp. 91–97

[8] Song, Y., Yin, J., Bu, W.*, et al.*: 'Effect of electrode materials on breakdown of Al_2O_3/Pi films'. IEEE 9th Int. Conf. on the Properties and Applications of Dielectric Materials, Harbin, China, July 2009, pp. 823–825

[9] Jones, T.I.: 'Mercury electrodes for measurements on solid dielectrics at radio frequencies', *Inst. Electr. Eng. – Proc. Wirel. Sect. Inst.*, 1934, **9**, (25), pp. 58–65

[10] Lane, J.W., Seferis, J.C., Bachmann, M.A.: 'Dielectric studies of the cure of epoxy matrix systems', *Polymer*, 1986, **31**, (5), pp. 1155–1167

[11] Pawar, M.S., Sutar, M.A., Maddani, K.I.*, et al.*: 'Improvement in electrochemical performance of spray deposited V_2O_5 thin film electrode by anodization', *Mater. Today, Proc.*, 2017, **4**, (2), pp. 3549–3556

[12] Kim, H.S., Gilmer, D.C., Campbell, S.A.*, et al.*: 'Leakage current and electrical breakdown in metal-organic chemical vapor deposited TiO_2 dielectrics on silicon substrates', *Appl. Phys. Lett.*, 1996, **69**, (25), pp. 3860–3862

[13] Ho, P.S., Hahn, P.O., Bartha, J.W.*, et al.*: 'Chemical bonding and reaction at metal polymer interfaces', *J. Vac. Sci. Technol. A.*, 1985, **3**, (3), pp. 739–745

[14] de Saint-Aubin, C., Rosset, S., Schlatter, S.*, et al.*: 'High-cycle electromechanical aging of dielectric elastomer actuators with carbon-based electrodes', *Smart Mater. Struct.*, 2018, **27**, (7), p. 074002

[15] Suriani, A.B., Nurhafizah, M.D., Mohamed, A.*, et al.*: 'Highly conductive electrodes of graphene oxide/natural rubber latex-based electrodes by using a hyper-branched surfactant', *Mater. Des.*, 2016, **99**, pp. 174–181

[16] Sau, K., Chaki, T., Khastgir, D.: 'The effect of compressive strain and stress on electrical conductivity of conductive rubber composites', *Rub. Chem. Technol.*, 2000, **73**, (2), pp. 310–324

[17] Packard, H.: 'Dielectric constant measurement of solid materials', Application Note 380-1, 1989

[18] Chavez, P.P.: 'Accurate Complex permittivity measurement with two-electrode contact-free apparatus', *IEEE Trans. Dielectr. Electr. Insul.*, 2018, **25**, (4), pp. 1470–1478

[19] Vykhodtsev, A.V., Kordi, B., Oliver, D.R.: 'Sensitivity analysis of a parallel-platemethod for measuring the dielectric permittivity of high-voltage insulating materials', *High Volt.*, 2017, **2**, (3), pp. 200–204

[20] Zhou, Y., Zhang, C., Li, W.*, et al.*: 'Correction of contact free measurement in outdoor insulation diagnostics'. 2016 Int. Conf. on Condition Monitoring and Diagnosis (CMD), Xi'an, China, September 2016, pp. 360–363

[21] Xu, X., Bengtsson, T., Blennow, J.*, et al.*: 'Correction of geometric influence in permittivity determination'. Proc. of the Nordic Insulation Symp., Trondheim, Norway, June 2013, pp. 71–74

[22] Yuan, C., Xie, C., Li, L.*, et al.*: 'Dielectric response characterization of in-service aged sheds of (U) HVDC silicone rubber composite insulators', *IEEE Trans. Dielectr. Electr. Insul.*, 2016, **23**, (3), pp. 1418–1426

[23] Hao, J., Xu, X., Taylor, N.: 'An electrode setup for non-contact dielectric response measurement'. Proc. of the Nordic Insulation Symp., Tampere, Finland, June 2019, pp. 88–93

[24] Freye, C., Jenau, F.: 'Model-based accuracy enhancements for guarded conductivity measurements: determination of effective electrode areas utilising numerical field simulation', *High Volt.*, 2018, **3**, (3), pp. 217–225